World Journal of Microbiology and Biotechnology (2022) 38:230
https://doi.org/10.1007/s11274-022-03405-2

ORIGINAL PAPER

Amikacin-loaded niosome nanoparticles improve amikacin activity against antibiotic-resistant *Klebsiella pneumoniae* strains

Mohamad Rahmati[1] · **Ebrahim Babapoor**[2] · **Mehrouz Dezfulian**[2]

Received: 30 October 2021 / Accepted: 27 August 2022 / Published online: 3 October 2022

Abstract

Amikacin is an aminoglycoside antibiotic used in drug-resistant bacterial infections. The spread of bacterial infections has become a severe concern for the treatment system because of the simultaneous drug resistance bacteria and SARS-CoV-2 hospitalized patients. One of the most common bacteria in the development of drug resistance is *Klebsiella* strains, which is a severe threat due to the possibility of biofilm production. In this regard, recent nanotechnology studies have proposed using nanocarriers as a practical proposal to improve the performance of antibiotics and combat drug resistance. Among drug nanocarriers, niosomes are considered for their absorption mechanism, drug coverage, and biocompatibility. In this study, niosomal formulations were synthesized by the thin-layer method. After optimizing the synthesized niosomes, their properties were evaluated in terms of stability and drug release rate. The toxicity of the optimal formulation was then analyzed. The effect of free amikacin and amikacin encapsulated in niosome on biofilm inhibition were compared in multi-drug resistant isolated *Klebsiella* strains, and the *mrkD* gene expression was calculated. The MIC and MBC were measured for the free drug and amikacin loaded in the noisome. The particle size of synthesized amikacin-loaded niosomes ranged from 175.2 to 248.3 nm. The results showed that the amount of lipid and the molar ratio of tween 60 to span 60 has a positive effect on particle size, while the molar ratio of surfactant to cholesterol has a negative effect. The highest release rate in amikacin-loaded niosomes is visible in the first 8 h, and then a slower release occurs up to 72 h. The cytotoxicity induced by amikacin-loaded niosome is significantly less than the cytotoxicity of free amikacin in HFF cells (***$p < 0.001$, **$p < 0.01$). The *mrkD* mRNA expression level in the studied strains was significantly reduced after treatment with niosome-containing amikacin compared to free amikacin (***$p < 0.001$). It was confirmed that in the presence of the niosome, the amikacin antibacterial activity increased while the concentration of the drug used decreased, the formation of biofilm inhibited, and reduced antibiotics resistance in MDR *Klebsiella* strains.

Keywords Amikacin · Antibiotic-resistance · *Klebsiella pneumoniae* · Niosome

Introduction

Klebsiella pneumoniae is one of the gram-negative bacteria with a high frequency of multi-drug resistance that causes infection in hospitalized patients, especially in SARS-CoV-2 (severe acute respiratory syndrome coronavirus 2) patients (Arcari et al. 2021)(Serra-Burriel et al. 2020)(Vivas et al. 2019). *Klebsiella* is a gram-negative, immobile, oxidase-negative, opportunistic pathogen and has a polysaccharide capsule. This opportunistic bacterium cause pneumonia, septicemia, and urinary tract infections in hospitalized patients. *Klebsiella pneumoniae* showed increasing obtain multi-drug resistance genes which cause difficult cure this nosocomial infection. It displayed broadly multi-drug resistance to the routine antibiotics, including extended-spectrum

✉ Mehrouz Dezfulian
dezfoulian@kiau.ac.ir; dezfulianmehr@gmail.com

Mohamad Rahmati
mohamad_drv@yahoo.com

Ebrahim Babapoor
e_babapoor@yahoo.com

[1] Department of Microbiology, Karaj Branch, Islamic Azad University, Karaj, Iran

[2] Biotechnology Research Center, Karaj Branch, Islamic Azad University, Karaj, Iran

beta-lactams, fluoroquinolones, aminoglycosides, trimethoprim, and sulfamethoxazole. The gene profile reported in MDR *Klebsiella pneumoniae* included blaSHV, blaCTX-M, blaTEM, blaOXA, and blaNDM beta-lactamase genes, class 1 integrons gene cassette, and the outer membrane protein gene *ompK36* and *ompA*, the *fim* (Type 1 fimbriae), *mrk* (Type 3 fimbriae) and *ecp* (E. coli common pilus) genes. These genes are the most reported in MDR *Klebsiella pneumoniae* strains (Flores-Valdez et al. 2021)(Lev et al. 2018) (Kumar et al. 2011).

Biofilm production is one of the reasons for the drug resistance of bacteria (Provenzani et al. 2020). In order to form a biofilm, most strains of this bacterium form type 3 fimbriae to attach to different cells and extracellular surfaces. Type 3 fimbriae consists of two components, major fimbriae (MrkA) and adhesive (MrkD) (Paczosa and Mecsas 2016) (D. et al. 2001). According to research, the presence of MrkD adhesive is essential for growth on collagen-containing surfaces (Jagnow and Clegg 2003)(Schroll et al. 2010). Biofilm production also increases their ability to survive in harsh environments in the host and is responsible for chronic and persistent infections (Wang et al. 2016). One of the antibiotics used to treat drug-resistant bacteria is amikacin. Amikacin is an aminoglycoside antibiotic that blocks the translation by binding to the small subunit of the bacterial ribosome. It inhibits protein synthesis by irreversibly binding to 16S prokaryotic ribosome rRNA and altering ribosome structure (Polat and Tapisiz 2018) (Marsot et al. 2017). The urinary system staves off with an average *t½* elim in plasma of 2.3 h (range 2.2–2.5 h) in patients with normal renal function(Routledge and Hutchings 2013). The administration dose of amikacin is usually based on the weight. Amikacin exhibits toxic side effects like the other aminoglycosides, such as nephrotoxicity and damage to the eighth cranial nerve. That caused a lack of balance and the loss of hearing. The administration of amikacin for multiple-daily dose should be < 30 mg/L (Routledge and Hutchings 2013) and > 10 mg/L (Routledge and Hutchings 2013). A concentration > 32 mg/L is a potentially toxic concentration. Amikacin showed the most resistance to aminoglycoside modifying enzymes compared to the other aminoglycosides(Routledge and Hutchings 2013). Amikacin's entrance into the *K. pneumonia* has an important impact on MDR due to amikacin resistance caused by the decrease of its uptake by *K. pneumonia* (Murray and Moellering 1982).

Niosomes are among the most widely used nanocarriers in drug delivery containing amphipathic lipids and nonionic surfactants. They are composed of one or more dense layers and encapsulate water-soluble and fat-soluble drugs (Saini et al. 2021). Niosomes are nonionic surfactant nanoparticles that have improved liposome properties. The advantage of niosomes is membrane formation by nonionic surfactants instead of phospholipids (which have been used in liposomes), increasing its stability and disinclination to oxidation and decreasing its cost. In addition, niosomes have a neutral charge and can be stored at room temperature. Niosome particles have successfully shown different routes for administration, such as intranasal, oral, ocular, dermal, and intravenous. It was first introduced for cosmetic application, but its osmotic behavior, biocompatible function, and nontoxic and non-inflammation properties are used as a drug delivery vehicle (Bartelds et al. 2018) (Marianecci et al. 2014). Niosomes are amphipathic compounds, and a hydrophobic membrane entraps their inner aqueous core. This hydrophobic membrane has high water permeability and neutral charge; therefore, it is easily fused to the cell membrane to deliver hydrophobic and hydrophilic drug compounds (Abdelkader et al. 2012).

These advantages caused us to choose niosome as a vehicle for the delivery of amikacin in this study.

Since multi-drug resistance in *Klebsiella pneumoniae* is a global and growing challenge, in this study, we attempt to synthesize niosomal structures containing the antibiotic amikacin and its effect on *Klebsiella pneumoniae* multidrug-resistant isolates into an effective treatment system for dealing with infectious diseases caused by this phenomenon.

Material and methods

Bacterial strains

Klebsiella pneumoniae ATCC 13,884 was used as a reference strain. In this study, 100 samples, including urine, wounds, cerebrospinal fluid, blood, and sputum, were collected from Tehran hospitals, among which 48 K. *pneumoniae* were identified (n = 48). The criterion for selection and collection of samples was the hospital laboratory report related to antibiotic resistance. Identification and isolation of *K. pneumoniae* strain were performed using biochemical tests such as SIM, TSI, MR-VP, urea, citrate, and oxidase (All the media used were taken from HiMedia Laboratories Pvt Ltd, India). The samples were collected according to the protocol of the ethics committee of Islamic Azad University Branch Karaj under IR.IAU.K.REC.1396.103, and IR.IAU.K.REC.1396.102 codes.

Optimization of amikacin-loaded niosome by experimental design

The effect of independent variables (lipid mmol, the molar ratio of surfactant: cholesterol, and the molar ratio of span 60: twin 60) on physicochemical properties of amikacin-loaded niosome by optimal design using Design-Expert 7.0.10 software (Stat-Ease Inc., USA) was done (Table 1).

Table 1 Different levels for variables in the Box–Behnken design optimization

Level	− 1	0	+ 1
A (Lipid, µmol)	200	250	300
B (Surfactant: Cholesterol, molar ratio)	0.5	1	2
C (Span60:Tween60, molar ratio)	75:25	50:50	25:75

In addition, the effect of the specified variables on size, polydispersity index (PDI), and encapsulation efficiency percent (EE%) is presented in Table 2. The optimal formulation with the smallest size and PDI range with the highest EE% was selected to continue the studies.

Preparation of amikacin- Loaded niosomes

The niosomes containing amikacin were synthesized based on the thin-film hydration method (Thabet et al. 2022). In this method, the weight amounts of span 60 and tween 60 with cholesterol are dissolved in chloroform solution (all from Sigma Aldrich, USA) and evaporated under vacuum at 60 ℃ by rotary evaporator (1 h, 120 rpm) (Heidolph Instruments, Germany). Next, hydration of the formed film was performed using 1 mg/ml of amikacin (Tehran-Darou, Iran) solution in phosphate buffer (PBS) (pH 7.2, one h, 120 rpm). Finally, the compositions prepared for 7 min were sonicated using a probe sonicator (Hielscher up50H ultrasonic processor, Germany). The samples were kept at 4 ℃ for further investigations.

Size, morphology, and polydispersity of index (PDI)

The morphology of blank and niosome-containing amikacin was examined by scanning electron microscopy (SEM) (Akbarzadeh et al. 2020). Evaluation of mean particle size, polydispersity index (PDI), and size dispersion of synthesized formulations was performed by dynamic light scattering (DLS) technique with Malvern Zeta Sizer (Malvern Instrument, U.K.) at room temperature. For this purpose, the 1: 100 sample suspension was first diluted in deionized water. A sample drop is then spread on a conductive film such as aluminum and dried at room temperature.

Entrapment efficiency

The rate of entrapment efficiency for synthesized formulations was specified by determining the amount of non-entrapped amikacin and amikacin trapped in the niosomes by the ultrafiltration method. Such that 1 ml of the niosomes encapsulated amikacin was centrifuged for 1 h at 4 ℃ (14,000×*g*). The amount of amikacin per sample was determined by calculating the maximum absorption of the supernatant at 520 nm. The percentage of EE was measured dependent on the following formula:

EE% = (Total amount of initial amikacin entrapped into the niosomes – the amount of free amikacin) / total amount of amikacin × 100.

Table 2 Design of experiments using Box–Behnken method to optimize the niosomal formulation of Amikacin

Run	Levels of independent variables			Dependent variables		
	Lipid, µmol	Surfactant: cholesterol, molar ratio	Span60:Tween60, molar ratio	Average size (nm)	PDI	Entrapment efficiency (EE) (%)
1	1	− 1	0	284.3	0.319	57.34
2	0	1	− 1	209.5	0.287	52.25
3	− 1	1	0	207.4	0.142	53.23
4	0	0	0	189.2	0.159	57.42
5	1	0	− 1	197.4	0.253	58.24
6	0	0	0	183.5	0.184	56.49
7	0	0	0	175.6	0.166	54.3
8	0	− 1	1	280.4	0.379	54.85
9	− 1	0	− 1	175.2	0.188	53.12
10	− 1	− 1	0	248.9	0.291	55.79
11	0	− 1	− 1	220.6	0.334	49.41
12	1	0	1	271.4	0.369	67.23
13	1	1	0	182.3	0.157	62.75
14	0	1	1	232.4	0.283	64.49
15	− 1	0	1	242.9	0.315	60.21

Fourier-transform infrared spectroscopy (FT-IR)

Fourier Transform Infrared Spectroscopy (Spectrum Two, USA.) was employed to investigate the interaction between amikacin and niosome components. For this purpose, the lyophilized sample was combined with KBr buffer, and FTIR analyzes were performed carefully at room temperature in the scanning range of 4000 to 400 cm^{-1} at a constant resolution of 4 cm^{-1}.

In-vitro release study of amikacin from niosome

The process of releasing amikacin from the structure of niosomes was investigated using 2 ml of amikacin solution and amikacin-loaded niosomes in a dialysis membrane (MWCO 12 KDa). The dialysis bags were then gently stirred (50 rpm) in 50 ml PBS buffer at 37 ℃ (pH 7.4). Then 1 ml of each sample was taken at regular intervals (1, 2, 4, 8, 24, 48, and 72 h), and the release rate of the samples was evaluated by spectrophotometry. In addition, the release mechanism of amikacin was investigated with different release kinetic profiles (Zero Order, First Order, Higuchi, and Korsmeyer–Peppas model). Meanwhile, the zero-order model is related to drug dissolution and is not dependent on concentration, while the first-order model expresses drug-dependent secretion. The Higuchi and Korsmeyer-Peppas models also represent drug secretion from polymer and matrix systems (Dash et al. 2010)(Mirzaie et al. 2020).

Stability studies

In order to evaluate the stability, size, PDI, and EE% of niosomal vesicles for optimal formulation containing amikacin in the time intervals of 0–14–30–60 days at 4 and 25 ℃ were measured.

Biofilm formation

Biofilm formation in *K. pneumoniae* isolated from samples was performed by the microtiter plate method (Stepanovic et al. 2000). According to the formula proposed by Stepanovic et al., the isolates were divided into entirely sticky, relatively sticky, weakly sticky, and non-sticky strains.

Detection of biofilm genes

By confirming the biofilm phenotype, genes involved in biofilm formation were determined using molecular methods and specific primers. First, DNA extraction was performed by the phenol–chloroform method. PCR method confirmed the presence of genes involved in biofilm formation. PCR reaction in 25 µl volume including 4.18 µl of deionized water, 2.5 µl of 10X PCR buffer, 1 µl of buffer, 2 mM MgCl, 1 µl of 0.5, 10 mM dNTPs of microliters of round primers with a concentration of 0.1, 20 pmol µmol Taq DNA polymerase and one microliter of the desired DNA were performed (Table 3). In summary, PCR reaction was performed in 30 cycles for 5 min at 94 ℃, one minute at 94 ℃, one minute at 55 ℃, one minute at 72 ℃, and 3 min at 72 ℃. PCR products were electrophoresed on 1% agarose gel for 30 min, stained with Ethidium bromide, and tested with a gel doc.

Anti-biofilm activity

Evaluation of inhibition of biofilm formation in two stages, before and after treatment (with amikacin and niosome containing amikacin), was performed by microtiter plate assay (Stepanovic et al. 2000).

Biofilm genes expression

The expression of biofilm-related genes in MDR *Klebsiella* strains was evaluated. Initially, for RNA extraction, isolates containing biofilm gene were first treated with sub-MIC concentrations of samples (free amikacin and amikacin loaded in niosome) for 24 h. Then the RNA was extracted using an extraction kit (Qiagen RNA, USA) according to the protocol. Then, cDNA synthesis from the extracted RNAs was performed by Quanti Tect Reverse Transcription kit (Qiagen kit, USA) using random hexamer primers. The concentration of synthesized cDNAs was determined and confirmed by nanodrop. Biofilm gene expression was assessed by Real-Time quantitative PCR (Applied Biosystem, UK). Compounds in a volume of 20 µl included 2 µl of cDNA, 10 pmol of each

Table 3 Primer sequences were used in PCR and RT-PCR

RmpA	For: ACTGGGCTACCTCTGCTTCA
	Rev: CTTGCATGAGCCATCTTTCA
fimH-1	For: GCCAACGTCTACGTTAACCTG
	Rev: ATATTTCACGGTGCCTGAAAA
mrkD	For: CCACCAACTATTCCCTCGAA
	Rev: ATGGAACCCACATCGACATT
arb	For: TGGGGCAAAGAGGCGCTG GAG
	Rev: CAGCCAGCGACACGGATTCTC
entB	For: CTGCTGGGAAAAGCGATTGTC
	Rev: AAGGCGACTCAGGAGTGGCTT
irP-1	For: TGAATCGCGGGTGTCTTATGC
	Rev: TCCCTCAATAAAGCCCACGCT
traT	For: GGTGTGGTGCGATGAGCACAG
	Rev: CACGGTTCAGCCATCCCTGAG
AcrAB	For: ATCAGCGGCCGGATTGGTAAA
	Rev: CGGGTTCGGGAAAATAGCGCG

primer, and 10 µl of Mastermix containing cyber green, which was performed on the ABI step one device United States. The *gmk* (guanylate kinase) gene was also used as an internal control. Relative expression of the studied genes was measured using the ΔΔCT method. Then, Rest software was used to calculate the amount of gene expression and draw the relevant graphs. Finally, expression analysis was performed by relative measurement of mRNA expression compared to the standard strain of *Klebsiella pneumoniae* (ATCC 25,923).

Cytotoxicity study

To determine the cytotoxicity of the samples (amikacin solution, niosome containing amikacin, and blank niosome) by MTT [(3- (4, 5-dimethylthiazol-2-yl)-2, 5- diphenyl-tetrazolium bromide] test, HFF cells (Human Foreskin Fibroblast cell line) from Pasteur Institute of Iran were used. First, the HFF cells were placed in a 96-well plate (10,000 cells per well) containing RPMI-1640 complete medium at 37 ℃ (5% CO2). The implanted cells were then exposed to different concentrations of free and loaded amikacin in the niosome, and after incubation, 20 µl of MTT solution (5 mg/ml) was added to each well with PBS buffer. After 3 h of incubation, the cell culture medium was replaced with 100 µl of DMSO, and the adsorption rate of each well was determined with a microplate reader (570 nm) (AccuReader, Metertech, Taiwan). The following formula also calculated the percentage of cell viability:

Cell viability % = (OD570 sample / OD570 control) *100.

Minimum inhibitory and bactericidal concentration (MIC & MBC)

MICs (Minimum inhibitory concentrations) and sub-MIC for studied *Klebsiella pneumoniae* strains exposed to free amikacin and niosome containing amikacin were confirmed using Clinical Laboratory Standard Institute (CLSI) broth microdilution method (Wikler 2006).

In addition, to determine MBC (minimum antibacterial concentration), 10 µl of each well was spread on Mueller Hinton agar (HiMedia Pvt Ltd, India) and incubated at 37 ℃ overnight. Then, by counting the colonies, MBC was reported as the lowest concentration of samples, resulting in a 99.9% reduction in initial inoculations.

Statistical analysis

Statistical calculations of this study were performed by SPSS software version 21. The one-way ANOVA was used to analyze the Real-Time PCR data, and statistical significance was considered P-value < 0.05.

Results

Physicochemical characterization of amikacin-loaded niosomes

In this study, the molar ratio of surfactant: cholesterol, tween 60: span 60, and lipid content were considered independent variables for optimizing responses (size, PDI, and EE%). The observed optimal responses for the studied independent variables were compared with the predicted values in the models, and a statistically significant coefficient has analyzed in the models.

The results presented in Table 4 show the values of the responses after the experiment.

Particle size analysis

As shown in Table 4, the particle size of amikacin-loaded niosomes ranged from 175.2 to 248.3 nm. According to the reported results, the best model for nanoparticle size was quadratic and statistically significant ($p < 0.05$). The model was considered significant since its p-value is below 0.05. Table 5 also presents the ANOVA analysis, showing that independent variables B and C affect particle size ($p < 0.05$). Table 6 summarizes the response size regression analysis to fit the quadratic model.

The plots shown in Fig. 1 show the interactions of independent variables (lipid content, the molar ratio of surfactant: cholesterol, and molar ratio of tween 60: span 60) on particle size. As shown in Fig. 1, the amount of lipid and the molar ratio of tween 60 to span 60 has a positive effect on particle size, while the molar ratio of surfactant to cholesterol has a negative effect.

Polydispersity index analysis

The polydispersity index (PDI) of amikacin-loaded niosomes ranged from 0.142 to 0.379; as listed in Table 4, the PDI statistical analyzes are presented in Tables 7 and 8. The response is polynomial and fitted to a quadratic model. The data in Table 7 show the effect of independent variables on PDI, and Table 8 shows the correlation of the PDI regression analysis summary with the quadratic model. Based on the presented results, the significant effect of B and C independent variables on PDI is evident ($p < 0.05$). In addition, the graphs in Fig. 2 confirm the significant role of the molar ratio of surfactant: cholesterol and the molar ratio of tween 60: span 60 on PDI, which show a negative effect and a positive effect on PDI, respectively.

Table 4 Design of experiments using response surface methodology (RSM) to optimize the niosomal formulation of Amikacin

Run	Levels of independent variables			Dependent variables		
	Lipid, µmol	Surfactant: cholesterol, molar ratio	Span60:Tween60, molar ratio	Average size (nm)	PDI	Entrapment efficiency (EE) (%)
1	1	− 1	0	284.3	0.319	57.34
2	0	1	− 1	209.5	0.287	52.25
3	− 1	1	0	207.4	0.142	53.23
4	0	0	0	189.2	0.159	57.42
5	1	0	− 1	197.4	0.253	58.24
6	0	0	0	183.5	0.184	56.49
7	0	0	0	175.6	0.166	54.3
8	0	− 1	1	280.4	0.379	54.85
9	− 1	0	− 1	175.2	0.188	53.12
10	− 1	− 1	0	248.9	0.291	55.79
11	0	− 1	− 1	220.6	0.334	49.41
12	1	0	1	271.4	0.369	67.23
13	1	1	0	182.3	0.157	62.75
14	0	1	1	232.4	0.283	64.49
15	− 1	0	1	242.9	0.315	60.21

Table 5 Analysis of variance for the quadratic polynomial model for size

Source	Sum of squares	Degree of freedom	Mean square	F-value	P-value	Evaluation
Model	18,775.78	9	2086.20	6.43	0.0271	Significant
A	465.13	1	465.13	1.43	0.2849	
B	5130.85	1	5130.85	15.81	0.0106	
C	6294.42	1	6294.42	19.39	0.0070	
AB	915.06	1	915.06	2.82	0.1540	
AC	9.92	1	9.92	0.031	0.8681	
BC	340.40	1	340.40	1.05	0.3528	
A^2	1064.46	1	1064.46	3.28	0.1299	
B^2	3543.54	1	3543.54	10.92	0.0214	
C^2	1783.69	1	1783.69	5.50	0.0660	

Table 6 Summary results of regression analysis for responses size, for fitting to quadratic model

Quadratic model	R^2	Adjusted R^2	Adeq Precision	SD	%CV	Lack of fit
	0.9204	0.7772	7.856	18.02	8.19	0.0850

Regression equations of the fitted model: Particle Size $= +182.77 + 7.62 \times A - 25.33 \times B + 28.05 \times C - 15.12 \times A \times B + 1.57 \times A \times C - 9.22 \times B \times C + 16.98 \times A^2 + 30.98 \times B^2 + 21.98 \times C^2$

Entrapment efficiency analysis

The entrapment efficiency (as mentioned before) for synthesized formulations was specified by determining the amount of non-entrapped amikacin and amikacin trapped in the niosomes by the ultrafiltration method.

Based on Table 4, the percentage of entrapment efficiency for the prepared formulations is 49.41–67.23%. In addition, the results in Table 9 report that all three independent variables (lipid content, the molar ratio of surfactant: cholesterol, and the molar ratio of tween 60: span 60) have a significant effect on EE% ($p < 0.05$). The fitted model was statistically significant (p value < 0.05). Table 10 also illustrates the regression equation for EE%. As shown in Fig. 3, the graphs confirm the significant and positive effect of lipid content, the molar ratio of tween

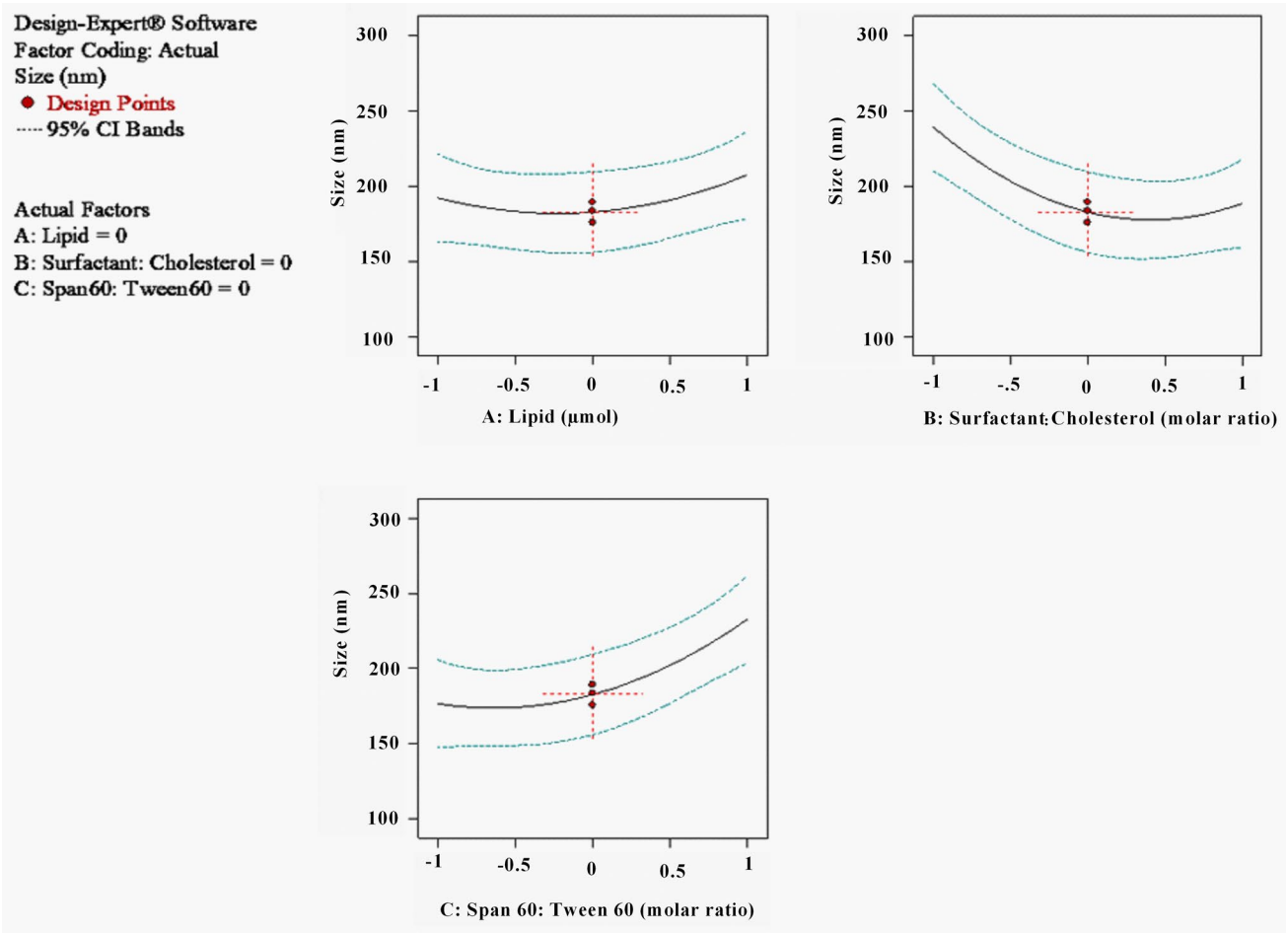

Fig. 1 Box–Behnken method for average diameter as a function of the parameters

Table 7 Analysis of variance for the quadratic polynomial model for PDI

Source	Sum of squares	Degree of freedom	Mean square	F-value	P-value	Evaluation
Model	0.085	9	9.419E-003	4.86	0.0481	Significant
A	3.281E-003	1	3.281E-003	1.69	0.2498	
B	0.026	1	0.026	13.30	0.0148	
C	0.010	1	0.010	5.21	0.0714	
AB	4.225E-005	1	4.225E-005	0.022	0.8883	
AC	3.025E-005	1	3.025E-005	0.016	0.9054	
BC	6.003E-004	1	6.003E-004	0.31	0.6017	
A^2	3.019E-004	1	3.019E-004	0.16	0.7093	
B^2	8.700E-003	1	8.700E-003	4.49	0.0876	
C^2	0.039	1	0.039	20.05	0.0065	

Table 8 Summary results of PDI regression analysis, for fitting to quadratic model

Quadratic model	R^2	Adjusted R^2	Adeq precision	SD	%CV	Lack of fit
	0.8957	0.7130	7.563	0.044	17.25	0.0511

Regression equations of the fitted model: $PDI = +0.170 + 0.020 \times A - 0.057 \times B + 0.036 \times C - 3.250E-003 \times A \times B - 2.750E-003 \times A \times C - 0.012 \times B \times C + 9.042E-003 \times A^2 + 0.049 \times B^2 + 0.100 \times C^2$

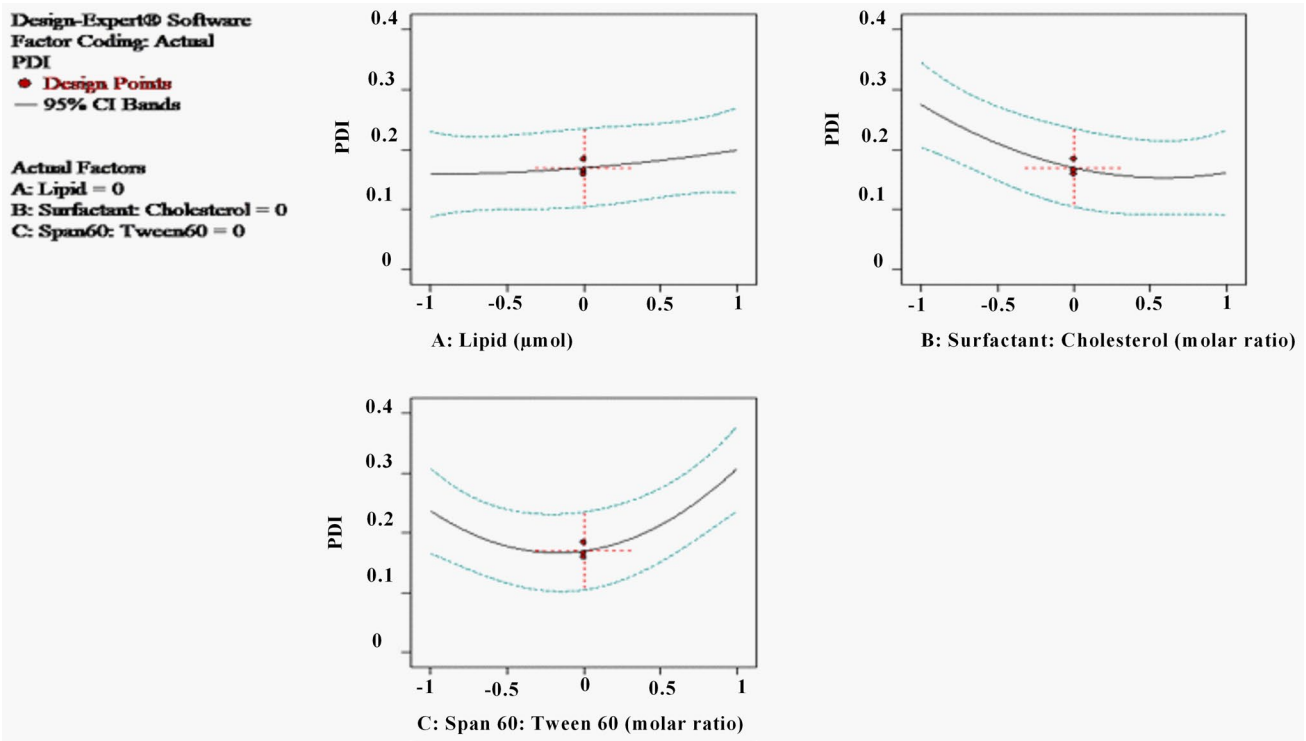

Fig. 2 Box–Behnken method for PDI as a function of the parameters

Table 9 Analysis of variance for the quadratic polynomial model for EE

Source	Sum of squares	Degree of freedom	Mean square	F-value	P-value	Evaluation
Model	311.54	9	34.62	10.07	0.0102	Significant
A	67.34	1	67.34	19.59	0.0069	
B	29.38	1	29.38	8.55	0.0329	
C	142.47	1	142.47	41.45	0.0013	
AB	15.88	1	15.88	4.62	0.0843	
AC	0.90	1	0.90	0.26	0.6302	
BC	11.56	1	11.56	3.36	0.1261	
A^2	29.55	1	29.55	8.60	0.0326	
B^2	9.71	1	9.71	2.82	0.1537	
C^2	2.37	1	2.37	0.69	0.4441	

Table 10 Summary results of EE regression analysis, for fitting to quadratic model

Quadratic model	R^2	Adjusted R^2	Adeq precision	SD	%CV	Lack of fit
	0.9477	0.8536	10.888	1.85	3.24	0.4126

Regression equations of the fitted model:EE $= +56.07 + 2.90 \times A + 1.92 \times B + 4.22 \times C + 1.99 \times A \times B + 0.47 \times A \times C\ 1.70 \times B \times C + 2.83 \times A^2 - 1.62 \times B^2 + 0.80 \times C^2$

60 to span 60, and the negative and significant effect of the molar ratio of surfactant: cholesterol, respectively. The regression analysis results of different responses to check the model's validity for predicting responses show a logical agreement between R2 and R2 (Tables 6, 8, 10). Also, sufficient accuracy for all responses is more than 4, which indicates a suitable signal-to-noise ratio (Shaker et al. 2015).

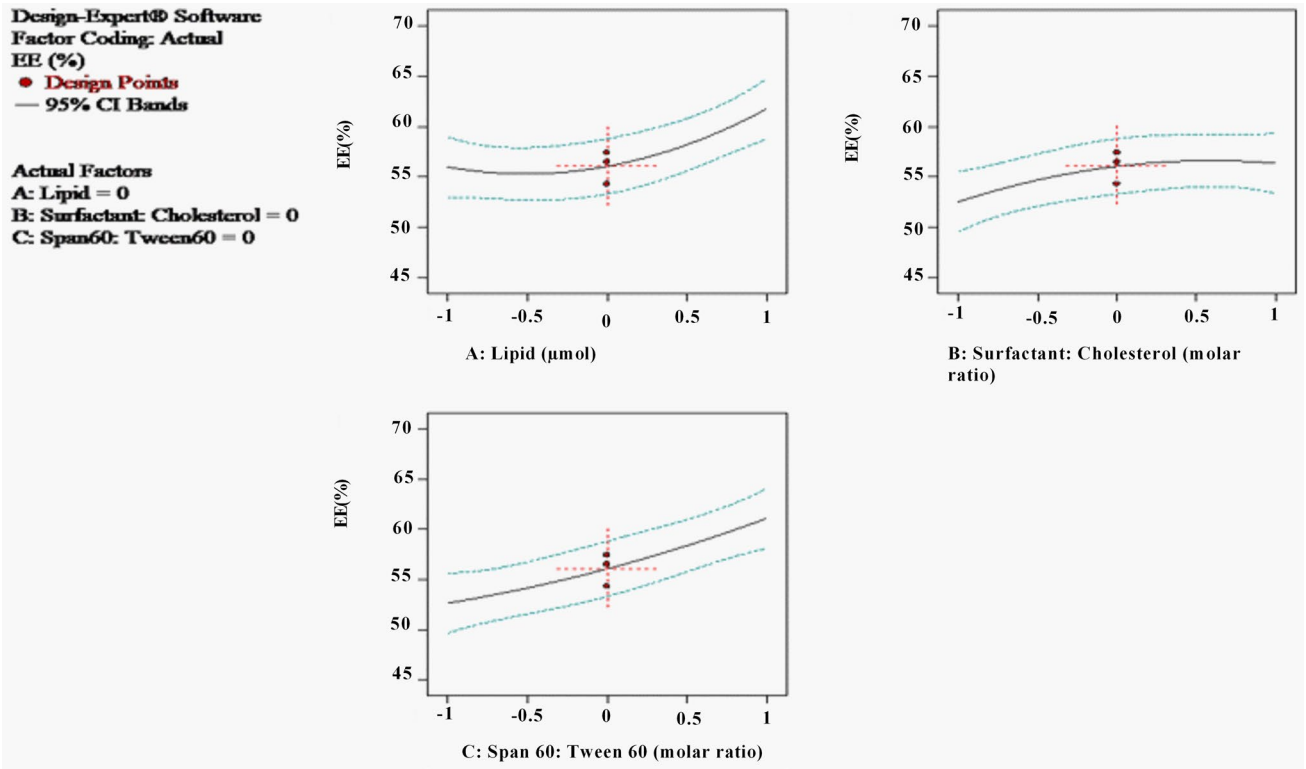

Fig. 3 Box–Behnken method for encapsulation efficiency (EE) function of the parameters

Data optimization

For data optimization, the effect of independent variables (lipid mmol, the molar ratio of surfactant: cholesterol, and molar ratio of span 60: twin 60) on physicochemical properties of amikacin loaded niosome and the effect of the specified variables on size, polydispersity index (PDI), and entrapment efficiency percent (EE%) by using Design-Expert 7.0.10 software (Stat-Ease Inc., USA) was done. The optimal formulation with the smallest size and PDI range with the highest EE% was selected to continue the studies.

According to the optimal conditions for the responses, the optimal performance of the conditions for all three responses was reported to be about 0.821, which was acceptable and indicated the validity of the experimental design method used. Optimal conditions were determined by considering the minimum particle size, limited PDI, and maximum entrapment efficiency. As a result, optimal formulations were synthesized (Table 11). The particle size, PDI, and EE were 196.26 nm, 0.184, and 64.27%, respectively. The observed responses from the experimental data were proportional to the predicted responses, and no significant differences were observed. Therefore, the optimized formulation was used for subsequent experiments (Table 11).

Table 11 The optimized responses obtained by Box–Behnken method and the experimental data for the same responses under the optimum conditions

Parameter	Predicted by Box–Behnken	Experimental data
Average size (nm)	196.269	178.27 ± 8.19
PDI	0.184	0.156 ± 0.011
Entrapment efficiency (EE) (%)	64.270	61.44 ± 0.69

Morphology of optimized niosomes encapsulated amikacin

As Fig. 4 shows, the morphological study and size distribution of the optimized niosome synthesized was performed by scanning electron microscopy (SEM) and dynamic light scattering (DLS), respectively. The image obtained from the synthesized niosomes shows a spherical and uniform morphology with a smooth surface. The diameter of niosomes was less than 40 nm, and there was also no accumulation in the synthesized and prepared niosomes.

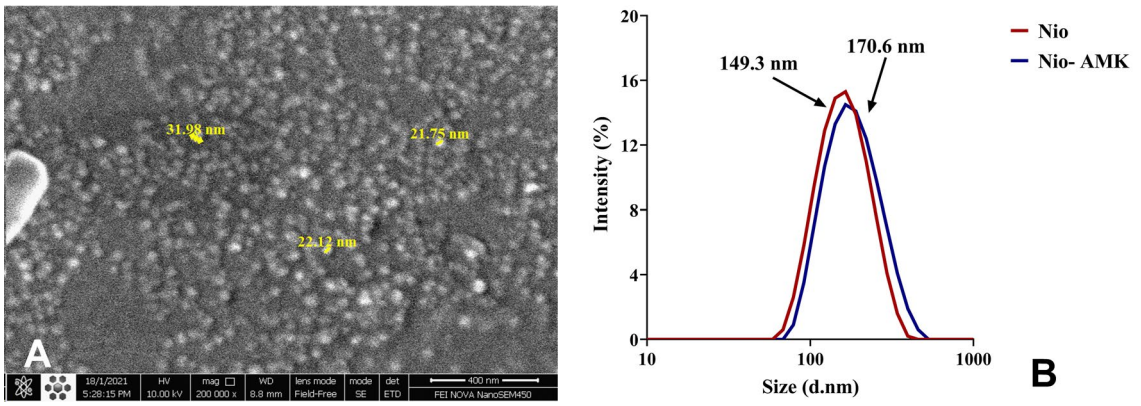

Fig. 4 Morphological determination of optimized formulation. **A** SEM (Scanning electron microscopy), **B** dynamic light scattering (DLS)

Fourier Transform Infrared (FTIR) analysis

FTIR analysis was used to confirm the presence of amikacin in the structure of the niosome containing amikacin. Figure 5a shows the FTIR spectrum of Tween 60, and several specific peaks in this spectrum are observable, including C–O stretching at 1117 cm^{-1}, C = O stretching at 1730 cm^{-1}, C–H stretching in the region of 2860–3907 cm^{-1}, and the OH stretching at 3452 cm^{-1}. Figure 5b demonstrates the FTIR spectrum of Span 60. The spectrum's bands can be assigned to C−O stretching at 1162 cm^{-1}, C−H stretching at 2852–2917 cm^{-1}, and the OH stretching at 3400 cm^{-1}. The FTIR pattern for Cholesterol (Fig. 5c) demonstrates various characteristic peaks, including C = O stretching at 1717 cm^{-1}, C−H stretching in the region of 2800–2890 cm^{-1}, OH stretching at 3398 cm^{-1}, CH2 bending, and CH2 deformation in the region of 1025–1364 cm^{-1}, C−C stretching an aromatic ring of 1455 cm^{-1}, and the C = C stretching at 1664 cm^{-1}. Figure 5d demonstrates the FTIR spectrum of the blank niosome. This spectrum's bands can be assigned to C−O stretching at 1110 cm^{-1}, C = O stretching at 1736 cm^{-1}, C−H stretching at 2858–2923 cm^{-1}, and OH stretching at 3406 cm^{-1}, and the aliphatic C-N stretching in the region of 1000–1292 cm^{-1}. Also, Fig. 5e shows the FTIR spectrum of amikacin, and specific peaks in this spectrum are observable, including N−H stretching in the region of 500–619 cm − 1, C−N stretching vibration at 1089 cm^{-1}, Amid I and II in the range of 1532 and 1624 cm^{-1}, C−H stretching in the range of 2900–3000 cm^{-1} and Stretching vibration of O–H and N–H at 3491 cm^{-1}. Eventually, with the addition of amikacin to the niosome, an amide group band appeared in the 1530 cm^{-1} region. This displacement was relative to the amikacin's amide, which could confirm the presence of the drug amikacin in the structure of the niosome. It was a link between the drug and the structure of the niosome (Fig. 5f).

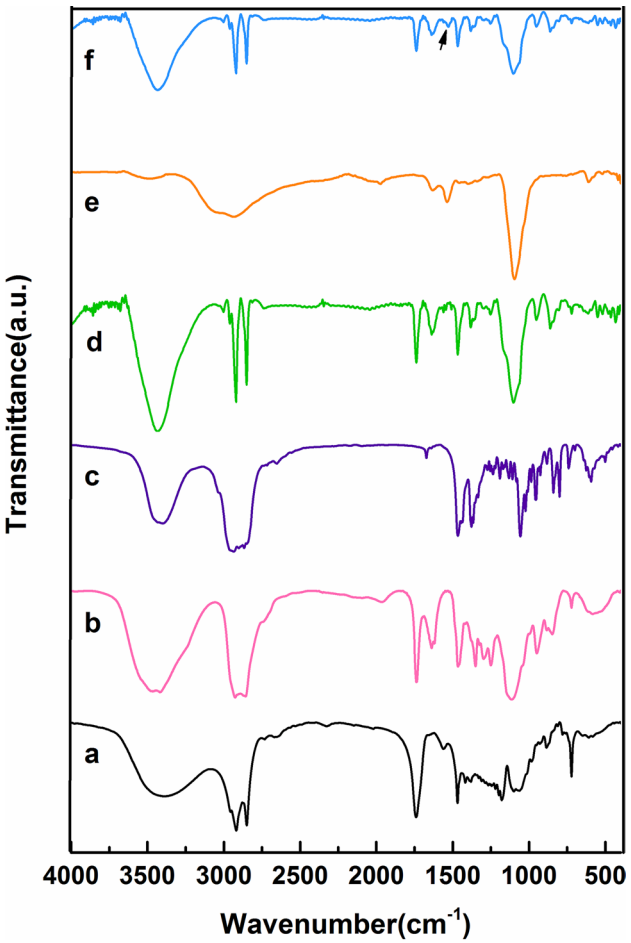

Fig. 5 **a** Tween 60, **b** Span 60, **c** Cholesterol, **d** Niosome, **e** Amikacin, f) Niosome containing amikacin

In vitro drug release profile and kinetics studies

A dialysis membrane was used to assess the release rate profile of amikacin. The results showed that in the first

8 h, the highest release rate is visible, and then a slower release occurs up to 72 h (Fig. 6). According to the results presented in Fig. 6, amikacin loaded in the niosomes can reduce the intensity of initial release and allow the drug release process to be controlled compared to the solution form of amikacin. On average, in the first 8 h, release for free amikacin and amikacin loaded in the niosome was reported to be 69% and 41%, respectively. Also, the release rate of amikacin from the optimal formulation of niosome for 72 h was 71% on average.

The release kinetic of amikacin from the niosome is presented in Table 12. According to the data presented in Table 12, the best kinetic model for free amikacin is First-Order, which represents concentration-dependent release. In addition, Korsmeyer-Peppas has been reported to have the best release kinetics for niosome-containing amikacin (Akbarzadeh et al. 2021).

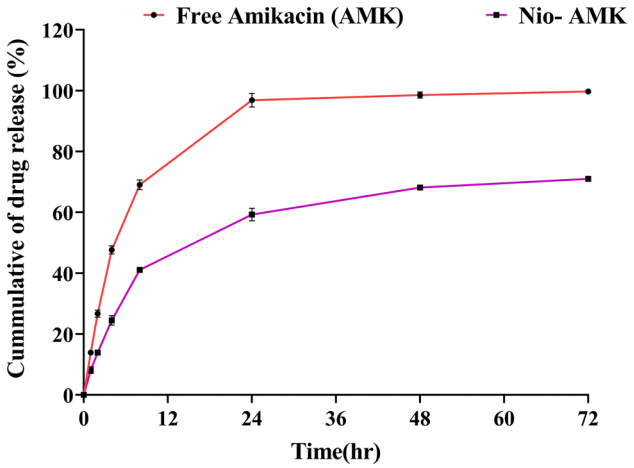

Fig. 6 In vitro drug release profile of amikacin from Niosome at 37 °C

Physical stability studies for amikacin loaded niosome

This study was performed by measuring the characteristics of niosomes, including size, PDF, and entrapment efficiency. As shown in Fig. 7, the synthesized niosomal formulations' stability was analyzed at 0, 14, 30, and 60 days at 4 ± 2 and 25 ± 2 ℃. The presented results confirm that over time (for two months), the size and PDI for niosomes increase significantly ($p < 0.05$) while the percentage of entrapment efficiency decreases significantly ($p < 0.05$). However, this process occurs more slowly at 4 ± 2 ℃ compared to 25 ± 2 ℃. Therefore, according to Fig. 7, the formulations stored at 4 ± 2 ℃ showed better stability compared to 25 ± 2 ℃.

Anti-biofilm Activity

The results of biofilm formation in the studied strains of *K. pneumoniae* bacterium by microtiter method are shown in Fig. 8. The results of this test show that the formation of biofilm in MDR *K. pneumoniae* strains treated with niosome-containing amikacin is significantly lower than in the pathogenic strains treated with free amikacin (Fig. 9) (***$p < 0.001$).

PCR amplification of biofilm-related genes

Figure 10 shows the results of PCR amplification of biofilm-related genes in MDR *K. pneumoniae* strains. PCR amplification of genes yielded an amplicon of 385 bp, 180 bp, 312 bp, 288 bp, 636 bp, 266 bp, 238 bp, and 535 bp for *entb*, *FimH*, *AcrAB*, *traT*, *arb*, *mrkD*, *irp-1*, *rmpA* genes, respectively.

mrkD gene expression

The results reported in Fig. 11 show that the *mrkD* mRNA expression level in the studied strains was significantly reduced after treatment with niosome-containing amikacin

Table 12 The kinetic release models and the parameters obtained for optimum niosomal formulation

Release model	Equation	R^2	
		Nio-AMK (pH 7.4–37 °C)	Free Amikacin (AMK) (pH 7.4–37 °C)
Zero-order	$C_t = C_0 + K_0 t$	$R^2 = 0.7724$	$R^2 = 0.6473$
Korsmeyer-Peppas*	$M_t/M = K_t^n$	$R^2 = 0.9361$	$R^2 = 0.8786$
		n = 0.5033*	n = 0.4395*
First-order	$LogC = LogC0 + K_t/2.303$	$R^2 = 0.8632$	$R^2 = 0.9487$
Higuchi	$Q = K_H \sqrt{t}$	$R^2 = 0.9102$	$R^2 = 0.8153$

*Diffusion or release exponent

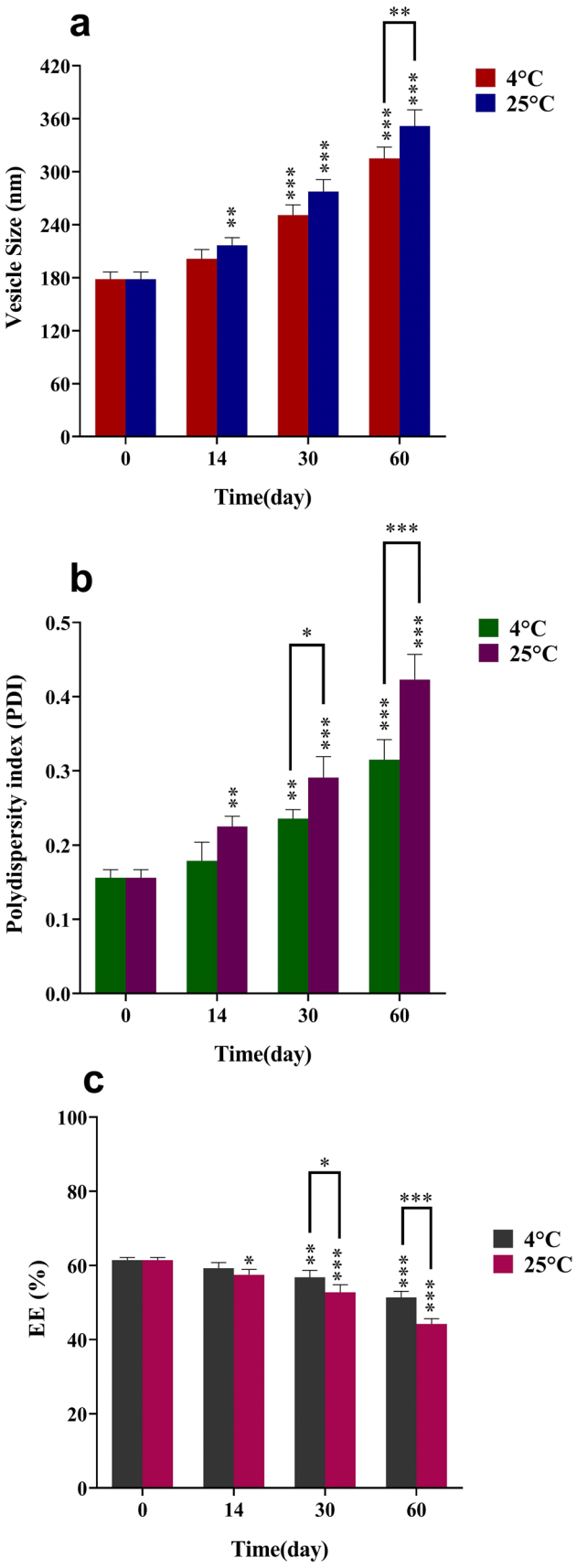

Fig. 7 Stability of optimum amikacin loaded niosomes stored during 60 days of storage at 4 ± 2 °C and 25 ± 2 °C, (*p-value < 0.05, **p-value < 0.01, and ***p-value < 0.001)

compared to free amikacin (***$p < 0.001$). Decreased expression of the *mrkD* gene in the presence of amikacin-loaded niosome indicates the proper functioning of the synthesized drug nanocarriers against biofilm structure formation.

Determination of MIC and MBC

The MIC and MBC for free amikacin and amikacin loaded in the niosome against MDR *K. pneumoniae* strains are presented in Tables 13 and 14. Examining the results presented in Tables 13 and 14 confirms that amikacin loaded in the niosome is more potent than free amikacin. Therefore the MIC values of encapsulated amikacin were lower than the free amikacin. The MIC values decreased from 100/50 ± 0.0 to 12.5/6.25 ± 0.0 and the 25/12.5 ± 0.0 to 3.125/1.56 ± 0.0 in the presence of amikacin loaded niosome. Also, the MBC values have been reduced from 200/100 ± 0.0 to 25/12.5 ± 0.0 and 50/25 ± 0.0 to 3.125/1.56 ± 0.0 due to niosome containing amikacin.

Cytotoxicity study

Cell viability was assessed at different concentrations of free amikacin and amikacin-loaded niosome in HFF cells (Fig. 12). The results show that the cytotoxicity induced by amikacin-loaded niosome is significantly less than the cytotoxicity of free amikacin (***$p < 0.001$, **$p < 0.01$). In addition, no significant toxicity resulted from cell treatment with empty niosomes. The nontoxic effects of the free niosomes and amikacin-loaded niosomes on HFF cells viability in all concentrations were the same as previously reported (Piri-Gharaghie et al. 2022).

Discussion

Klebsiella pneumoniae can lead to pneumonia in hospitalized patients and people with weakened immune systems (Aris et al. 2020) (Bandick et al. 2020) (Marsot et al. 2017).

One of the antibiotics used to treat drug-resistant bacteria is amikacin because it can escape the attack of antibiotic-inactivating enzymes responsible for antibiotic resistance in bacteria. The effectiveness of amikacin against *Klebsiella pneumonia* increased dose-dependent manner (Singla et al. 2013). Therefore, various nanostructures were designed to increase amikacin penetration into bacterial cells.

The different amikacin- nanoparticles with different structures have been reported. The encapsulating of amikacin

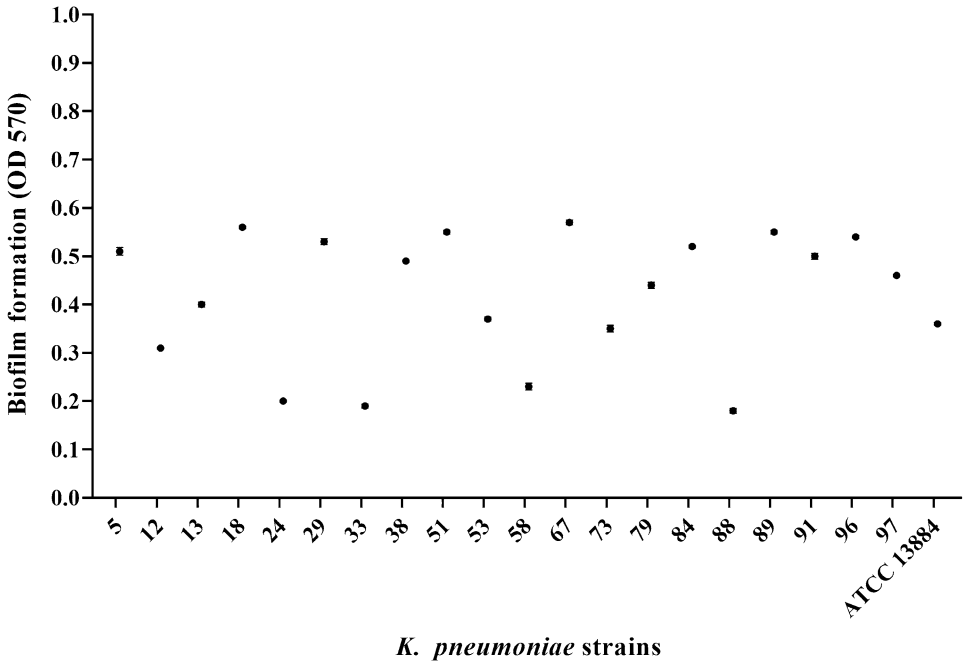

Fig. 8 Biofilm formation values (OD 570) of MDR *K. pneumoniae* strains

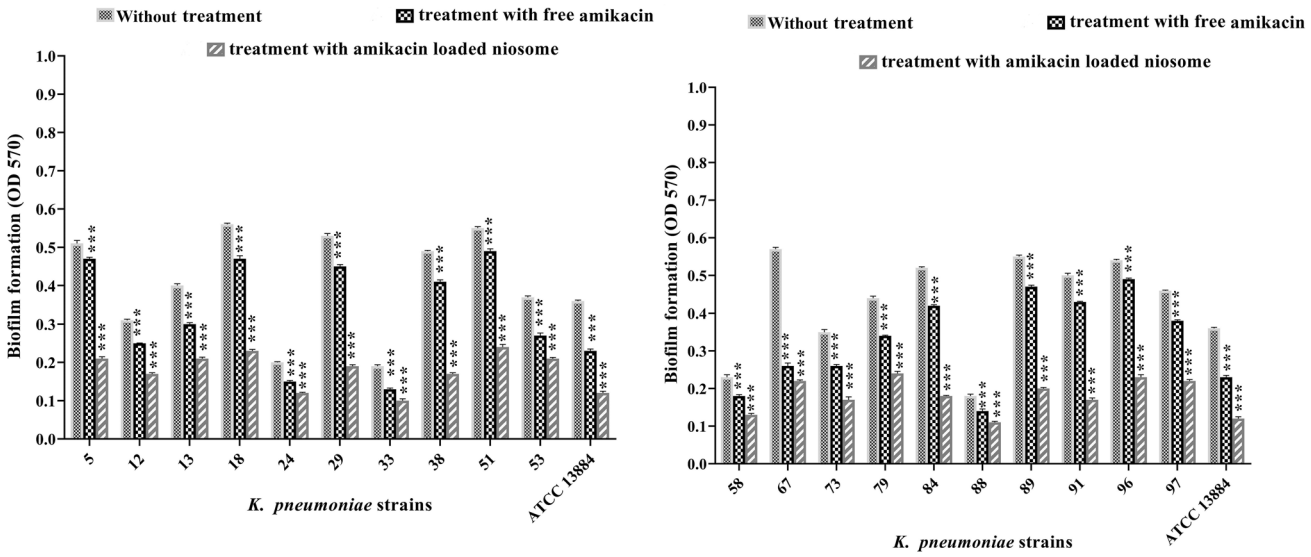

Fig. 9 Anti-biofilm activity of optimum prepared niosome encapsulated amikacin using microtiter plate. The biofilm formation was quantified for each bacterial strain, and 200 µl of bacterial suspension was added to each well of 96 well plates, of which three wells were assigned to treating amikacin, three wells for treating amikacin- noisome, and three wells for positive control without treatment. Three wells contain only 200 µl broth media culture as negative control wells. (*p-value < 0.05, **p-value < 0.01, and ***p-value < 0.001)

by using low-molecular-weight poly(lactic acid) (PLA) and poly(lactic acid-co-polyethylene glycol) (PLA-PEG), both supplemented with poly(vinyl alcohol) (PVA), was reported that the particle size was < 30 µm for long term release the MBC, MIC and, cytotoxicity was not determined (Glinka et al. 2021). Another amikacin- nanoparticle is the combination of gold nanostars (GNS) and amikacin, in which it is the minimum inhibitory concentration (MIC), and minimal bactericidal concentration (MBC) were 80 and 160 µM of GNS for all strains, respectively (Aguilera-Correa et al. 2022). Another is that coated gold nanoparticles reported that their binding to amikacin was mediated by trisodium citrate, polyvinylpolypyrrolidone, and Tween 20. Antibacterial activity has been studied in the zone of inhibition against Gram-positive (*S. aureus*) and Gram-negative (*E. coli*) bacterial strains. For *E. coli,* the zone of inhibition was

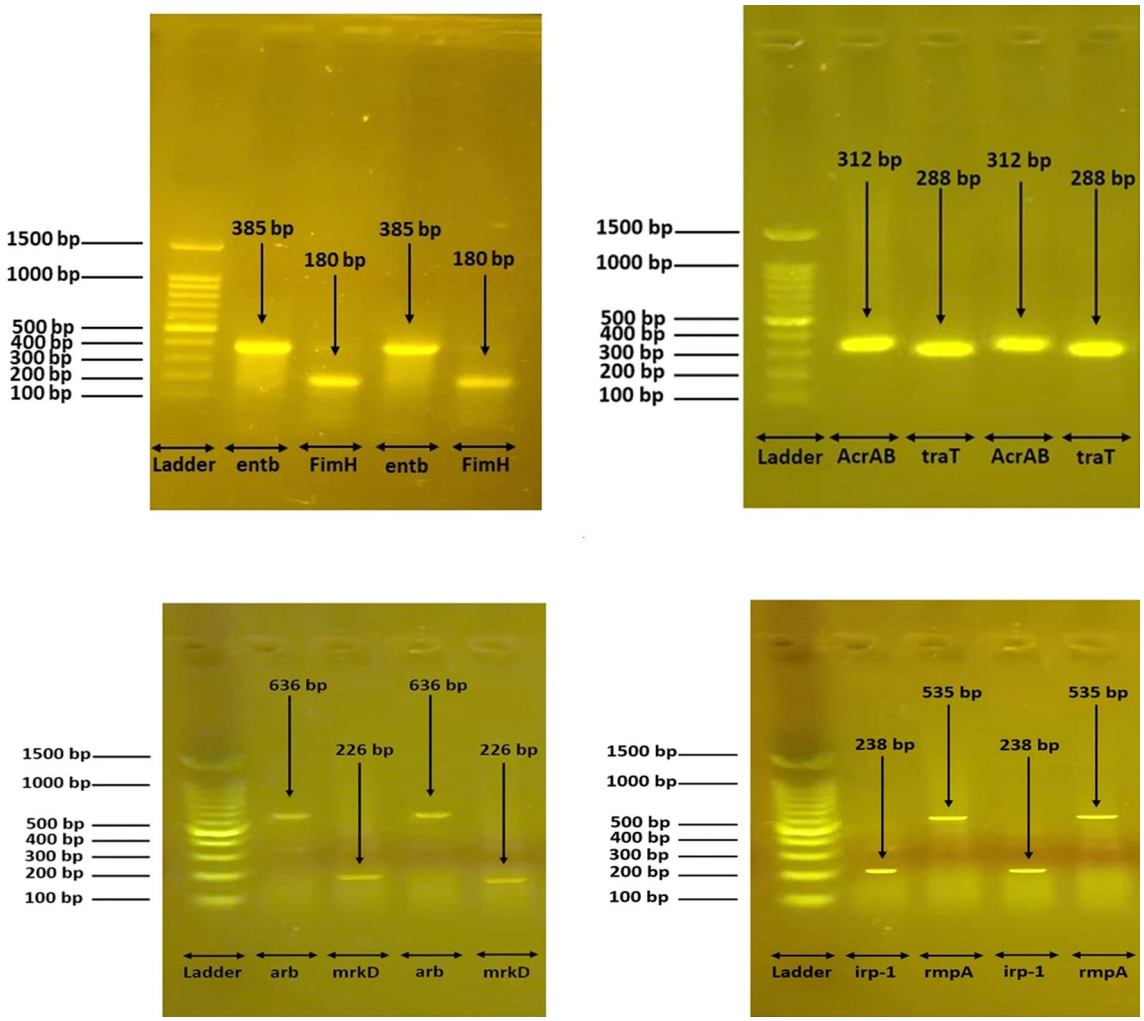

Fig. 10 PCR electrophoresis of *entb, FimH, AcrAB, traT, arb, mrkD, irp-1*, *rmpA* genes amplification

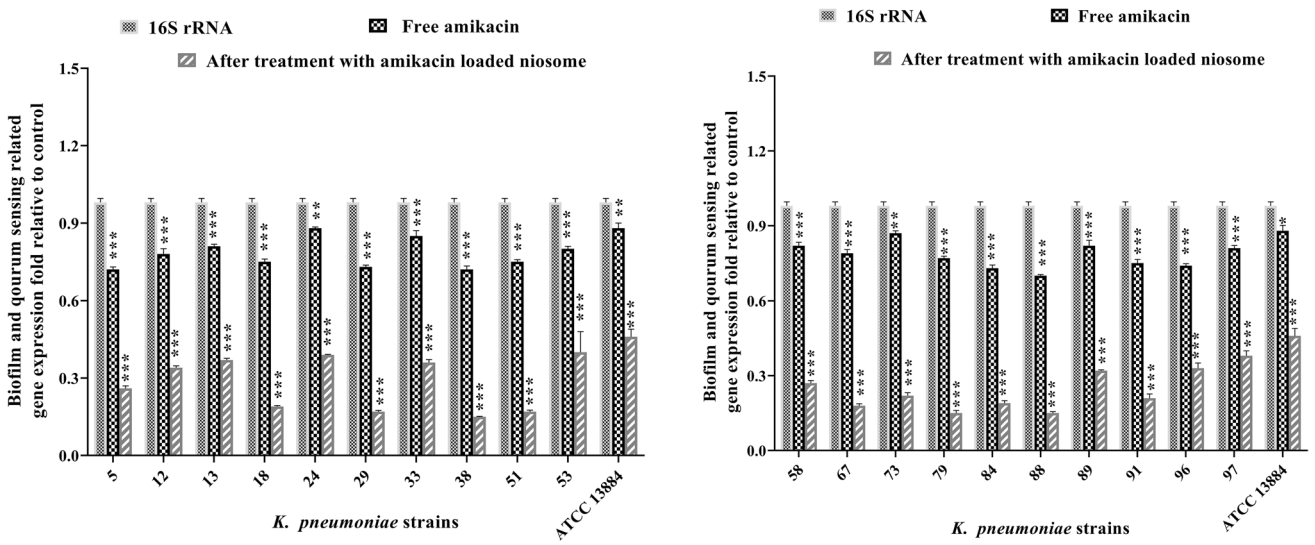

Fig. 11 *mrkD* gene relative expression in selected *K. pneumoniae* MDR strains is represented as fold difference between *mrkD* gene and *16S rRNA* gene following treatment (*p-value < 0.05, **p-value < 0.01, and ***p-value < 0.001)

Table 13 MIC and sub-MIC values of Amikacin and noisome encapsulated Amikacin against *K. pneumoniae* strains

K.P Strain no	MIC/sub-MIC values of free amikacin	MIC/sub-MIC values of amikacin loaded niosome
5	100/50 ± 0.0	25/12.5 ± 0.0
12	12.5/6.25 ± 0.0	3.125/1.56 ± 0.0
13	25/12.5 ± 0.0	12.5/6.25 ± 0.0
18	50/25 ± 0.0	6.25/3.125 ± 0.0
24	25/12.5 ± 0.0	3.125/1.56 ± 0.0
29	50/25 ± 0.0	6.25/3.156 ± 0.0
33	50/25 ± 0.0	12.5/6.25 ± 0.0
38	25/12.5 ± 0.0	6.25/3.125 ± 0.0
51	100/50 ± 0.0	12.5/6.25 ± 0.0
53	25/12.5 ± 0.0	3.125/1.56 ± 0.0
58	50/25 ± 0.0	6.25/3.125 ± 0.0
67	25/12.5 ± 0.0	12.5/6.25 ± 0.0
73	25/12.5 ± 0.0	6.25/3.125 ± 0.0
79	25/12.5 ± 0.0	6.25/3.125 ± 0.0
84	50/25 ± 0.0	3.125/1.56 ± 0.0
88	25/12.5 ± 0.0	3.125/1.56 ± 0.0
89	25/125 ± 0.0	12.5/6.25 ± 0.0
91	100/50 ± 0.0	25/12.5 ± 0.0
96	25/12.5 ± 0.0	6.25/3.125 ± 0.0
97	50/2.5 ± 0.0	3.125/1.56 ± 0.0

Table 14 MBC and sub-MBC values of Amikacin and noisome encapsulated Amikacin against *K. pneumoniae* strains

K.P Strain no	MBC/sub-MBC values of amikacin	MBC/sub-MBC values of amikacin loaded niosome
5	200/100 ± 0.0	50/25 ± 0.0
12	25/12.5 ± 0.0	6.25/3.125 ± 0.0
13	25/12.5 ± 0.0	25/12.5 ± 0.0
18	100/50 ± 0.0	12.5/6. 25 ± 0.0
24	50/25 ± 0.0	3.125/1.56 ± 0.0
29	50/25 ± 0.0	6.25/3.125 ± 0.0
33	100/50 ± 0.0	25/12.5 ± 0.0
38	50/25 ± 0.0	12.5/6.25 ± 0.0
51	200/100 ± 0.0	25/12.5 ± 0.0
53	50/25 ± 0.0	6.25/3.125 ± 0.0
58	100/50 ± 0.0	12.5/6.25 ± 0.0
67	50/25 ± 0.0	25/12.5 ± 0.0
73	50/25 ± 0.0	12.5/6.25 ± 0.0
79	25/12.5 ± 0.0	12.5/6.25 ± 0.0
84	100/50 ± 0.0	6.25/3.125 ± 0.0
88	50/25 ± 0.0	3.125/1.56 ± 0.0
89	50/25 ± 0.0	25/12.5 ± 0.0
91	100/50 ± 0.0	50/25 ± 0.0
96	50/25 ± 0.0	12.5/3.125 ± 0.0
97	100/50 ± 0.0	6.25/1.56 ± 0.0

enhanced from 8 to 13 mm, at 0.5 mM concentration. The AuNPs alone had no inhibitory effect on bacterial growth (63 µg/ml) (Kaur and Kumar 2022). The poly d, l-lactide-co-glycolide (PLGA)- amikacin for oral administration was synthesized, and their size was 260.3 nm. The MIC was reported 33.94 ± 0.98% within 1 h, but the tested microbial strains did not mention(Sabaeifard et al. 2016).

The combination of amikacin and the silver nanoparticles had a synergistic effect and demonstrated a decrease in MIC to the half on all tested *E.coli* and *Klebsiella* isolates (Desouky et al. 2020).

There is no evidence of cytotoxicity of the mentioned amikacin -nanoparticles and their inhibitory concentration on MDR *Klebsiella pneumoniae.* The niosomes are smaller than the mentioned nanoparticles and less toxic due to the nonionic surfactant with one hydrophobic tail (Bartelds et al. 2018) (Hajiahmadi et al. 2019).

In this study, the antibiotic amikacin was encapsulated in synthesized niosomal nanocarriers. The presence of span 60 and Tween 60 in the structure of synthesized niosomes creat stability and increases the entrapment efficiency of the drug (Hajiahmadi et al. 2019) (Lee et al. 2005). The particle size is the noteworthy feature in the efficiency of drug EE% and releases from the niosome, and the amount of the niosome constituents, such as cholesterol, play a role (Akbari et al. 2013). In a mixture, PDI represents a uniform size of the particles, which varies in the range of 0–1, and the particles of the same size are uniform. Therefore, homogeneous compounds have lower PDIs that are less prone to aggregation. With probe ultrasound, we can reduce the size and reach nano-sized niosomes (Pardakhty et al. 2007). These features enhanced the entrance of amikacin into the host cells and caused the accumulation of amikacin in the phagosome, which changed the distribution of antibiotics in the cells and reduced the amikacin cytotoxic effects in host cells that our findings confirm these findings.

As Fig. 4 shows, the size of the synthesized niosomes reported in the SEM image is smaller than the size obtained from DLS. The difference in size is because the image observed in SEM is for the dry and anhydrous sample, while in DLS, the size of the nanoparticles is displayed along with the surrounding water molecules and ions (Moghassemi et al. 2015).

Examination of the amikacin release profile at 37 ℃ and 0–72 h from the optimal niosome formulation indicates that the cumulative release is biphasic compared to free amikacin. The initial and rapid phase of amikacin release depends on the release of free amikacin or drug at the niosome surface, while the drug's passive and slow-release phase is related to release through the niosome layers(Lee et al. 2005). The mechanism of drug release is explained based on the linear form of different kinetic models for release data. An optimal kinetic model has a regression

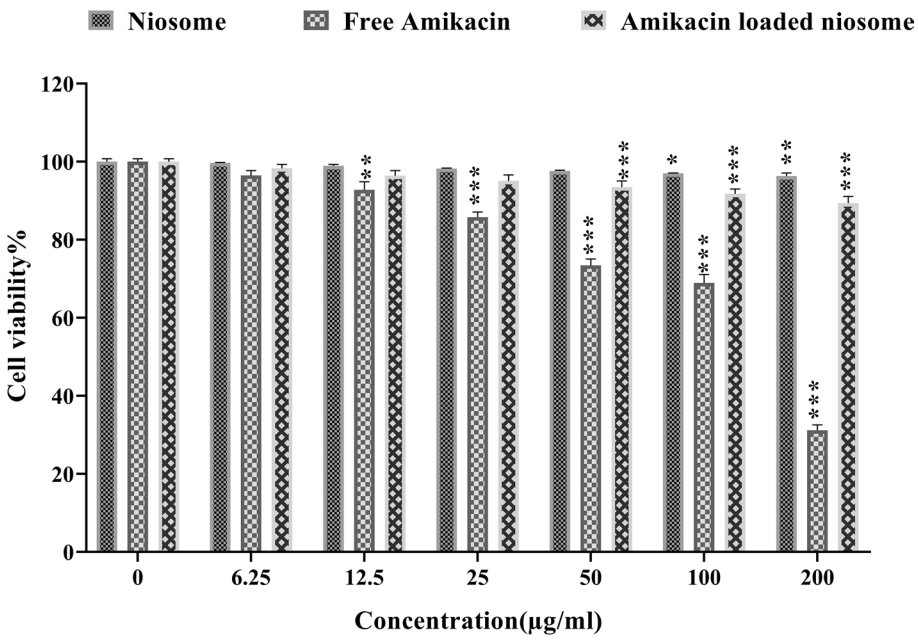

Fig. 12 Cell viability at different concentrations of free amikacin and amikacin loaded niosome in HFF cells

coefficient close to 1. Table 12 presents the kinetic and R2 data for each model and found that drug release is controlled by diffusion and erosion mechanisms (Manosroi et al. 2003). In addition, the measured n values indicate the secretion of the drug by Fickian diffusion release. In general, the evaluation of the amikacin release profile indicates an improvement in the drug release rate by using the niosome as the drug carrier, which also controls the duration of the drug by reducing its side effects of the drug(Cortesi et al. 2013).

Instability studies performed on optimal niosomal formulations it was shown that in the first two weeks of storage, the rate of change of size, PDI, and encapsulation efficiency for niosomes was slow. The bilayer membrane motility reduces at 4 ℃ in the niosome structure, but its size increases over time due to the fusion and accumulation of vesicles (Balasubramaniam et al. 2002). At high temperatures (25 ℃) compared to 4 ℃, the possibility of lipid fluidization in the vesicles' membrane is higher, leading to drug leakage. One of the essential compounds in the stability of niosomes is cholesterol, which can prevent membrane leakage (Fang et al. 2001).

The lack of proper uptake of amikacin into *Klebsiella pneumonia* was reported(Murray and Moellering 1982). The improvement of the effectiveness of amikacin- noisome against *Klebsiella pneumonia* confirmed the suggested possible mechanism of noisomes' antibacterial effects, including:

(a) The niosomes fluidize the bacterial cell membrane and increase membrane permeability to the drug.
(b) The adsorption of the niosomes vesicles and drug transfer enhance the antibiotic concentration in the bacterial cells.
(c) The noisome positively charged vesicles are attracted to the negatively charged bacteria and fusion between the noisome vesicles and bacterial membrane.
(d) The niosomes reduce biofilm formation even at drug concentrations much lower than the MIC due to the reduced number of viable cells (Abdelaziz et al. 2015).

The proper performance of antibiotics can be reduced due to the lack of proper penetration into bacterial cells. In this study, an optimal niosomal formulation containing amikacin was synthesized to evaluate the antibacterial and anti-biofilm effects against K. pneumoniae drug-resistant strains, which had a size of 178.2 nm, a PDI of 0.156, and EE% of 61.4. The MIC and MBC showed that the antibacterial activity of amikacin encapsulated in the niosome is much higher than free amikacin, which is applied following a lower concentration of the drug and therefore has fewer side effects. In studies on the toxicity of free amikacin, niosomes containing amikacin, and blank niosome, it was found that niosomes alone do not show significant toxicity, so any antibacterial activity is related to the presence of amikacin.

In this study, the expression of the *mrkD* gene of the studied strains was significantly (***$p < 0.001$) reduced in treated by the niosome- amikacin, which indicates the inhibition of biofilm formation in the bacterium (Fig. 10) (Jagnow and Clegg 2003).

Conclusion

In this study, we synthesized niosomes containing amikacin. The optimized noisome-amikacin structure provides stability and controls drug release for antibacterial function. The changed distribution of amikacin in the organelle of host cells showed non-toxicity to the HFF cells and simultaneously caused improved the uptake of antibiotics by *Klebsiella pneumonia*. The penetrance of noisome-amikacin into the bacterial cells significantly inhibited biofilm-related gene expression in drug-resistant *Klebsiella pneumonia*. Therefore, these nanostructures can treat chronic infections caused by drug-resistant *Klebsiella* bacteria and improve treatment.

Acknowledgements The authors gratefully acknowledge the laboratory staff that helped in this study.

Funding This research did not receive any specific grant from public, commercial, or not-for-profit sector funding agencies.

Declarations

Conflict of interest The authors declare no conflict of interest associated with the present manuscript.

References

Abdelaziz AA, Elbanna TE, Sonbol FI et al (2015) Optimization of niosomes for enhanced antibacterial activity and reduced bacterial resistance: in vitro and in vivo evaluation. Expert Opin Drug Deliv 12:163–180. https://doi.org/10.1517/17425247.2014.942639

Abdelkader H, Wu Z, Al-Kassas R, Alany RG (2012) Niosomes and discomes for ocular delivery of naltrexone hydrochloride: Morphological, rheological, spreading properties and photo-protective effects. Int J Pharm. https://doi.org/10.1016/j.ijpharm.2012.05.011

Aguilera-Correa JJ, García-Álvarez R, Mediero A et al (2022) Effect of gold nanostars plus amikacin against carbapenem-resistant *Klebsiella pneumoniae* biofilms. Biology 11(2):162. https://doi.org/10.3390/biology11020162

Akbari V, Abedi D, Pardakhty A, Sadeghi-Aliabadi H (2013) Ciprofloxacin nano-niosomes for targeting intracellular infections: an in vitro evaluation. J Nanoparticle Res. https://doi.org/10.1007/s11051-013-1556-y

Akbarzadeh I, Tavakkoli Yaraki M, Bourbour M et al (2020) Optimized doxycycline-loaded niosomal formulation for treatment of infection-associated prostate cancer: an in-vitro investigation. J Drug Deliv Sci Technol 57:101715. https://doi.org/10.1016/j.jddst.2020.101715

Akbarzadeh I, Keramati M, Azadi A et al (2021) Optimization, physicochemical characterization, and antimicrobial activity of a novel simvastatin nano-niosomal gel against *E. coli* and *S. aureus*. Chem Phys Lipids 234:105019. https://doi.org/10.1016/j.chemphyslip.2020.105019

Arcari G, Raponi G, Sacco F et al (2021) *Klebsiella pneumoniae* infections in COVID-19 patients: a 2-month retrospective analysis in an Italian hospital. Int J Antimicrob Agents 57:106245. https://doi.org/10.1016/j.ijantimicag.2020.106245

Aris P, Robatjazi S, Nikkhahi F, Amin Marashi SM (2020) Molecular mechanisms and prevalence of colistin resistance of *Klebsiella pneumoniae* in the Middle East region: a review over the last 5 years. J Glob Antimicrob Resist 22:625–630. https://doi.org/10.1016/j.jgar.2020.06.009

Balasubramaniam A, Anil Kumar V, Sadasivan Pillai K (2002) Formulation and in vivo evaluation of niosome-encapsulated daunorubicin hydrochloride. Drug Dev Ind Pharm 28:1181–1193. https://doi.org/10.1081/DDC-120015351

Bandick RG, Mousavi S, Bereswill S, Heimesaat MM (2020) Review of therapeutic options for infections with carbapenem-resistant *Klebsiella pneumoniae*. Eur J Microbiol Immunol (EuJMI) 10:115–124. https://doi.org/10.1556/1886.2020.00022

Bartelds R, Nematollahi MH, Pols T et al (2018) Niosomes, an alternative for liposomal delivery. PLoS ONE. https://doi.org/10.1371/journal.pone.0194179

Cortesi R, Ravani L, Rinaldi F et al (2013) Intranasal immunization in mice with nonionic surfactants vesicles containing HSV immunogens: a preliminary study as possible vaccine against genital herpes. Int J Pharm 440:229–237. https://doi.org/10.1016/j.ijpharm.2012.06.042

D OA, Jennifer L, Megan B, Steven C (2001) Type 3 fimbrial shaft (MrkA) of *Klebsiella pneumoniae*, but not the fimbrial adhesin (MrkD), facilitates biofilm formation. Infect Immun 69:5805–5812. https://doi.org/10.1128/IAI.69.9.5805-5812.2001

Dash S, Murthy PN, Nath L, Chowdhury P (2010) Kinetic modeling on drug release from controlled drug delivery systems. Acta Pol Pharm 67:217–223

Desouky EM, Shalaby MA, Gohar MK, Gerges MA (2020) Evaluation of antibacterial activity of silver nanoparticles against multidrug-resistant gram negative bacilli clinical isolates from Zagazig University hospitals. Microbes Infect Dis 1:15–23. https://doi.org/10.21608/mid.2020.27148.1003

Fang JY, Hong CT, Chiu WT, Wang YY (2001) Effect of liposomes and niosomes on skin permeation of enoxacin. Int J Pharm 219:61–72. https://doi.org/10.1016/s0378-5173(01)00627-5

Flores-Valdez M, Ares MA, Rosales-Reyes R et al (2021) Whole genome sequencing of pediatric *Klebsiella pneumoniae* strains reveals important insights into their virulence-associated traits. Front Microbiol 2:71157. https://doi.org/10.3389/fmicb.2021.711577

Glinka M, Filatova K, Kucińska-Lipka J et al (2021) Encapsulation of amikacin into microparticles based on low-molecular-weight poly(lactic acid) and poly(lactic acid-co-polyethylene glycol). Mol Pharm 18:2986–2996. https://doi.org/10.1021/acs.molpharmaceut.1c00193

Hajiahmadi F, Alikhani MY, Shariatifar H et al (2019) The bactericidal effect of lysostaphin coupled with liposomal vancomycin as a dual combating system applied directly on methicillin-resistant *Staphylococcus aureus* infected skin wounds in mice. Int J Nanomedicine 14:5943–5955. https://doi.org/10.2147/IJN.S214521

Jagnow J, Clegg S (2003) *Klebsiella pneumoniae* MrkD-mediated biofilm formation on extracellular matrix- and collagen-coated surfaces. Microbiology 149:2397–2405. https://doi.org/10.1099/mic.0.26434-0

Kaur A, Kumar R (2022) Untangling the effect of surfactants as an intermediate at gold nanoparticle-antibiotic interface for enhanced bactericidal effect. ES Food Agrofor 7:30–40. https://doi.org/10.30919/esfaf563

Kumar V, Sun P, Vamathevan J et al (2011) Comparative genomics of *Klebsiella pneumoniae* strains with different antibiotic resistance profiles. Antimicrob Agents Chemother 55:4267–4276. https://doi.org/10.1128/AAC.00052-11

Lee S-C, Lee K-E, Kim J-J, Lim S-H (2005) The effect of cholesterol in the liposome bilayer on the stabilization of incorporated Retinol. J

Liposome Res 15:157–166. https://doi.org/10.1080/08982100500364131

Lev AI, Astashkin EI, Kislichkina AA et al (2018) Comparative analysis of *Klebsiella pneumoniae* strains isolated in 2012–2016 that differ by antibiotic resistance genes and virulence genes profiles. Pathog Glob Health 112:142–151. https://doi.org/10.1080/20477724.2018.1460949

Manosroi A, Wongtrakul P, Manosroi J et al (2003) Characterization of vesicles prepared with various nonionic surfactants mixed with cholesterol. Colloids Surfaces B Biointerfaces 30:129–138. https://doi.org/10.1016/S0927-7765(03)00080-8

Marianecci C, Di Marzio L, Rinaldi F et al (2014) Niosomes from 80s to present: the state of the art. Adv Colloid Interface Sci 205:187–206. https://doi.org/10.1016/j.cis.2013.11.018

Marsot A, Guilhaumou R, Riff C, Blin O (2017) Amikacin in critically Ill patients: a review of population pharmacokinetic studies. Clin Pharmacokinet 56:127–138. https://doi.org/10.1007/s40262-016-0428-x

Mirzaie A, Peirovi N, Akbarzadeh I et al (2020) Preparation and optimization of ciprofloxacin encapsulated niosomes: a new approach for enhanced antibacterial activity, biofilm inhibition and reduced antibiotic resistance in ciprofloxacin-resistant methicillin-resistance *Staphylococcus aureus*. Bioorg Chem 103:104231. https://doi.org/10.1016/j.bioorg.2020.104231

Moghassemi S, Parnian E, Hakamivala A et al (2015) Uptake and transport of insulin across intestinal membrane model using trimethyl chitosan coated insulin niosomes. Mater Sci Eng C Mater Biol Appl 46:333–340. https://doi.org/10.1016/j.msec.2014.10.070

Murray BE, Moellering RCJ (1982) In-vivo acquisition of two different types of aminoglycoside resistance by a single strain of *Klebsiella pneumoniae* causing severe infection. Ann Intern Med 96:176–180. https://doi.org/10.7326/0003-4819-96-2-176

Paczosa MK, Mecsas J (2016) *Klebsiella pneumoniae*: going on the offense with a strong defense. Microbiol Mol Biol Rev 80:629–661. https://doi.org/10.1128/MMBR.00078-15

Pardakhty A, Varshosaz J, Rouholamini A (2007) In vitro study of polyoxyethylene alkyl ether niosomes for delivery of insulin. Int J Pharm 328:130–141. https://doi.org/10.1016/j.ijpharm.2006.08.002

Piri-Gharaghie T, Jegargoshe-Shirin N, Saremi-Nouri S et al (2022) Effects of Imipenem-containing Niosome nanoparticles against high prevalence methicillin-resistant *Staphylococcus Epidermidis* biofilm formed. Sci Rep 12:5140. https://doi.org/10.1038/s41598-022-09195-9

Polat M, Tapisiz A (2018) Amikacin monotherapy for treatment of febrile urinary tract infection caused by extended-spectrum β-Lactamase-producing *Escherichia coli* in children. Pediatr Infect Dis J 37:378–379

Provenzani A, Hospodar AR, Meyer AL et al (2020) Multidrug-resistant gram-negative organisms: a review of recently approved antibiotics and novel pipeline agents. Int J Clin Pharm 42:1016–1025. https://doi.org/10.1007/s11096-020-01089-y

Routledge PA, Hutchings AD (2013) Therapeutic drug monitoring (TDM).The immunoassay handbook: Theory and applications of ligand binding, ELISA and Related Techniques. 945–962. https://doi.org/10.1016/B978-0-08-097037-0.00076-2

Sabaeifard P, Abdi-Ali A, Soudi MR et al (2016) Amikacin loaded PLGA nanoparticles against *Pseudomonas aeruginosa*. Eur J Pharm Sci 93:392–398. https://doi.org/10.1016/j.ejps.2016.08.049

Saini A, Panwar D, Panesar PS, Bera MB (2021) Encapsulation of functional ingredients in lipidic nanocarriers and antimicrobial applications: a review. Environ Chem Lett 19:1107–1134. https://doi.org/10.1007/s10311-020-01109-3

Schroll C, Barken KB, Krogfelt KA, Struve C (2010) Role of type 1 and type 3 fimbriae in *Klebsiella pneumoniae* biofilm formation. BMC Microbiol 10:179. https://doi.org/10.1186/1471-2180-10-179

Serra-Burriel M, Keys M, Campillo-Artero C et al (2020) Impact of multi-drug resistant bacteria on economic and clinical outcomes of healthcare-associated infections in adults: systematic review and meta-analysis. PLoS ONE 15:e0227139. https://doi.org/10.1371/journal.pone.0227139

Shaker DS, Shaker MA, Hanafy MS (2015) Cellular uptake, cytotoxicity and in-vivo evaluation of Tamoxifen citrate loaded niosomes. Int J Pharm 493:285–294. https://doi.org/10.1016/j.ijpharm.2015.07.041

Singla S, Harjai K, Chhibber S (2013) Susceptibility of different phases of biofilm of *Klebsiella pneumoniae* to three different antibiotics. J Antibiot (Tokyo) 66:61–66. https://doi.org/10.1038/ja.2012.101

Stepanovic S, Vukovic D, Dakic I et al (2000) A modified microtiter-plate test for quantification of staphylococcal biofilm formation. J Microbiol Methods 40:175–179. https://doi.org/10.1016/s0167-7012(00)00122-6

Thabet Y, Elsabahy M, Eissa NG (2022) Methods for preparation of niosomes: a focus on thin-film hydration method. Methods 199:9–15. https://doi.org/10.1016/j.ymeth.2021.05.004

Vivas R, Barbosa AAT, Dolabela SS, Jain S (2019) Multidrug-resistant bacteria and alternative methods to control them: an overview. Microb Drug Resist 25:890–908. https://doi.org/10.1089/mdr.2018.0319

Wang Q, Chang C-S, Pennini M et al (2016) Target-agnostic identification of functional monoclonal antibodies against *Klebsiella pneumoniae* multimeric MrkA fimbrial subunit. J Infect Dis 213:1800–1808. https://doi.org/10.1093/infdis/jiw021

Wikler MA (2006) Methods for dilution antimicrobial susceptibility tests for bacteria that grow aerobically: approved standard. CLSI 26:M7-A7